

## Washington University School of Medicine Digital Commons@Becker

---

### Open Access Publications

---

2018

# High-affinity interactions and signal transduction between A $\beta$ oligomers and TREM2

Christian B. Lessard  
*University of Florida*

Samuel L. Malnik  
*University of Florida*

Yingyue Zhou  
*Washington University School of Medicine in St. Louis*

Thomas B. Ladd  
*University of Florida*

Pedro E. Cruz  
*University of Florida*

*See next page for additional authors*

Follow this and additional works at: [https://digitalcommons.wustl.edu/open\\_access\\_pubs](https://digitalcommons.wustl.edu/open_access_pubs)

---

### Recommended Citation

Lessard, Christian B.; Malnik, Samuel L.; Zhou, Yingyue; Ladd, Thomas B.; Cruz, Pedro E.; Ran, Yong; Mahan, Thomas E.; Charabaty, Paramita; Holtzman, David M.; Ulrich, Jason D.; Colonna, Marco; and Golde, Todd E., "High-affinity interactions and signal transduction between A $\beta$  oligomers and TREM2." *EMBO Molecular Medicine*.10,11. e9027. (2018).  
[https://digitalcommons.wustl.edu/open\\_access\\_pubs/7365](https://digitalcommons.wustl.edu/open_access_pubs/7365)




This Open Access Publication is brought to you for free and open access by Digital Commons@Becker. It has been accepted for inclusion in Open Access Publications by an authorized administrator of Digital Commons@Becker. For more information, please contact [engeszer@wustl.edu](mailto:engeszer@wustl.edu).

---

**Authors**

Christian B. Lessard, Samuel L. Malnik, Yingyue Zhou, Thomas B. Ladd, Pedro E. Cruz, Yong Ran, Thomas E. Mahan, Paramita Charabaty, David M. Holtzman, Jason D. Ulrich, Marco Colonna, and Todd E. Golde

# High-affinity interactions and signal transduction between A $\beta$ oligomers and TREM2

Christian B Lessard<sup>1</sup>, Samuel L Malnik<sup>1</sup>, Yingyue Zhou<sup>2</sup>, Thomas B Ladd<sup>1</sup>, Pedro E Cruz<sup>1</sup>, Yong Ran<sup>1</sup> , Thomas E Mahan<sup>3</sup>, Paramita Chakrabaty<sup>1,4</sup>, David M Holtzman<sup>3</sup> , Jason D Ulrich<sup>3</sup>, Marco Colonna<sup>2</sup> & Todd E Golde<sup>1,4,\*</sup> 

## Abstract

Rare coding variants in the triggering receptor expressed on myeloid cells 2 (TREM2) are associated with increased risk for Alzheimer's disease (AD), but how they confer this risk remains uncertain. We assessed binding of TREM2, AD-associated TREM2 variants to various forms of A $\beta$  and APOE in multiple assays. TREM2 interacts directly with various forms of A $\beta$ , with highest affinity interactions observed between TREM2 and soluble A $\beta$ 42 oligomers. High-affinity binding of TREM2 to A $\beta$  oligomers is characterized by very slow dissociation. Pre-incubation with A $\beta$  is shown to block the interaction of APOE. In cellular assays, AD-associated variants of TREM2 reduced the amount of A $\beta$ 42 internalized, and in NFAT assay, the R47H and R62H variants decreased NFAT signaling activity in response to A $\beta$ 42. These studies demonstrate i) a high-affinity interaction between TREM2 and A $\beta$  oligomers that can block interaction with another TREM2 ligand and ii) that AD-associated TREM2 variants bind A $\beta$  with equivalent affinity but show loss of function in terms of signaling and A $\beta$  internalization.

**Keywords** Alzheimer's disease; amyloid; APOE; innate immune response; TREM2

**Subject Categories** Genetics, Gene Therapy & Genetic Disease; Neuroscience

**DOI** 10.15252/emmm.201809027 | Received 21 February 2018 | Revised 13 September 2018 | Accepted 17 September 2018 | Published online 19 October 2018

**EMBO Mol Med (2018) 10: e9027**

## Introduction

The most prevalent form of dementia, Alzheimer's disease (AD), is hypothesized to be triggered by accumulation of aggregated amyloid- $\beta$  (A $\beta$ ) followed by a "cascade-like" chain of events that includes induction of tauopathy, neurodegeneration, and alterations in innate immune signaling (Hardy & Selkoe, 2002; Musiek & Holtzman, 2015). The later feature is reflected by the presence of

a reactive astrocytosis, microgliosis, and increased level and accumulation of a variety of immune molecules. A more central role of the innate immune system and microglial cells in particular has emerged from genetic studies. These studies show that numerous loci encoding immune genes are associated with altered risk for AD. Even more compelling are data showing that coding variants in three different genes (*TREM2*, *PLCG2*, and *ABI3*), whose transcripts are expressed primarily in microglial cells in the brain, alter risk for AD (Golde *et al*, 2013; Jin *et al*, 2014; Sims *et al*, 2017). Despite these associations between the immune system and AD, there is little consensus as to how alterations in the immune system mechanistically alter AD risk. Modeling studies reveal a complex relationship between immune activation states, the proteinopathies found in AD, and neurodegeneration—a phenomenon we refer to as immunoproteostasis (Chakrabarty *et al*, 2015). Further, definitive insight into how genetic variations within immune loci that alter AD risk alter immune function has remained enigmatic. Further understanding of how genetic risk factors impact the immune function will be important to guide therapeutic development, that to date has largely focused on anti-inflammatory strategies (Chakrabarty *et al*, 2015).

The rare protein coding variants in TREM2, R47H, and R62H, which are reproducibly associated with increased risk for developing AD, are being intensively studied as these variants were the first coding variants in an innate immune gene that have been reproducibly shown to alter risk for AD (Cruchaga *et al*, 2013; Jin *et al*, 2015; Lill *et al*, 2015). Prior to association with AD, homozygous or compound heterozygous mutations in TREM2 had been identified in a disease called polycystic lipomembranous osteodysplasia with sclerosing leukoencephalopathy (PLOS) or Nasu-Hakola disease (Bianchin *et al*, 2006). PLOS is characterized by fractures, frontal lobe syndrome, and progressive presenile dementia beginning in the fourth decade. Numerous studies of the PLOS-associated TREM2 variants suggest that these variants are loss of function altering maturation and cell-surface expression of TREM2 (Paloneva *et al*, 2001, 2002). Both structural and cell biology studies of the AD TREM2 variants show they lie on the surface of the TREM2 ectodomain, possibly framing a binding pocket, whereas the PLOS

1 Center for Translational Research in Neurodegenerative Disease, Department of Neuroscience, University of Florida, Gainesville, FL, USA

2 Department of Pathology and Immunology, Washington University School of Medicine, St. Louis, MO, USA

3 Department of Neurology, Hope Center for Neurological Disorders, Knight ADRC, Washington University School of Medicine, St. Louis, MO, USA

4 McKnight Brain Institute, University of Florida, Gainesville, FL, USA

\*Corresponding author. Tel: +1 352 273 9458; Fax +1 352 294 5060; E-mail: tgolde@ufl.edu

variants are within the core structure (Kleinberger *et al*, 2014; Kober *et al*, 2016). Maturation studies demonstrate folding and maturation deficits induced by PLOSL-associated TREM2 variants, whereas the AD variants do not consistently show these same functional impairments. Notably, a DNA polymorphism within a DNase hypersensitive site 5' of TREM2, rs9357347-C, also associates with reduced AD risk and increased TREML1 and TREM2 levels (Carrasquillo *et al*, 2017). This variant is associated with decreased risk for AD, which would be consistent with the hypothesis that the coding variants in TREM2 associated with increased AD risk are partial loss of function.

TREM2 is a type I transmembrane glycoprotein that interacts with the transmembrane region of DAP12 (TYROBP) to mediate signaling events through DAP12's immunoreceptor tyrosine-based activation motif (ITAM) domain (Peng *et al*, 2010). The extracellular, immunoglobulin-like domain V type, domain of TREM2 is glycosylated and shows cell-surface localization. TREM2 is highly expressed in microglia and peripheral macrophages (Colonna & Wang, 2016). TREM2 is one member of a family of receptors that have diverged between mouse and humans. In both mouse and human, the family members are clustered within a single chromosomal region on chromosome 6. In the context of neurodegenerative disease, the other family members have not been intensively studied as they are typically expressed at much lower levels in the brain. Like many type I membrane receptors, TREM2 can undergo ectodomain shedding and subsequent intramembrane cleavage by  $\gamma$ -secretase (Wunderlich *et al*, 2013). The physiologic implications of these proteolytic cleavages remain unclear, though increased soluble TREM2 has been reported in the CSF of early-stage Alzheimer's disease (Suarez-Calvet *et al*, 2016), and study of a variant p.H157Y reported to be associated with AD in the Han Chinese population has been shown to increase ectodomain shedding (Jiang *et al*, 2016a; Schlepckow *et al*, 2017; Thornton *et al*, 2017). Enhanced shedding activity from the mutation p.H157Y located in the ectodomain cleavage site leads to a reduced cell-surface TREM2 and phagocytic activity (Schlepckow *et al*, 2017; Thornton *et al*, 2017).

TREM2 has been implicated in multiple functions including migration, survival and proliferation, cytokine release, and phagocytosis (Kleinberger *et al*, 2014; Ulrich & Holtzman, 2016; Yuan *et al*, 2016). TREM2 appears to be a promiscuous receptor and has been shown to interact with cellular debris, bacteria, anionic phospholipids, nucleic acids, and apolipoprotein E (APOE; Atagi *et al*, 2015; Bailey *et al*, 2015; Yeh *et al*, 2016; Kober & Brett, 2017; Song *et al*, 2017). Alterations in signaling and binding of TREM2 AD variants compared to wild-type (WT) TREM2 have been reported, though the pathogenic relevance of these alterations is not yet completely clear (Kleinberger *et al*, 2014; Kober *et al*, 2016). Mouse modeling studies show increased TREM2 expression in multiple models of neurodegenerative diseases, and TREM2-positive microglial cells appear to surround plaques in APP models (Jiang *et al*, 2014; Ulrich *et al*, 2014; Yuan *et al*, 2016; Jay *et al*, 2017). TREM2 also shows an altered distribution in microglia surrounding the amyloid plaque, with much of the TREM2 immunoreactivity localized within the plasma membrane of the microglial cells adjacent to the plaque. In TREM2 knockout mice crossed with APP, there are fewer microglial cells surrounding plaques and an increase in plaques with "specular" amyloid morphology as well as more neuritic dystrophy (Wang

*et al*, 2015, 2016). Such data have led to the hypothesis that TREM2 may regulate the interaction of microglia with plaques and protect other brain cells from toxicity.

In this study, we investigated whether TREM2 and its AD variants interact directly with A $\beta$ . We found no significant changes in the binding affinity between A $\beta$ 42 with TREM2 or the AD variants or with their mouse counterpart Trem2, Trem1, and Trem11. Despite this lack of difference in the binding affinity, we observed an attenuated activation of NFAT signaling and a reduced amount of A $\beta$ 42 internalized by cells expressing the TREM2 AD variants. We show that TREM2, TREM1 and TREML1 bind APOE and A $\beta$  variably. Our study reveals that the TREM2 and other family members can bind various forms of A $\beta$  and that A $\beta$  oligomers can induce signaling events. Further, our data are consistent with the hypothesis that AD risk variants in TREM2 induce a partial loss of function (Song *et al*, 2018), but do not directly alter binding affinity for either A $\beta$  or APOE.

## Results

### Soluble TREM2-Fc and soluble TREML1-Fc interact with A $\beta$ 42 fibrils

The ectodomain of TREM2 interacts with various ligands including bacterial liposaccharides and phospholipids. We explored whether TREM2 might interact with A $\beta$  and whether this interaction might be affected by the AD variants. We also analyzed mouse Trem2 in order to compare its relative binding ability to human TREM2. Initial studies focused on whether TREM2 could interact with fibrillar A $\beta$ 42 (fA $\beta$ ), using an A $\beta$ 42 pull-down assay we have previously validated (Chakrabarty *et al*, 2015). Conditioned media from transiently transfected HEK 293 cells expressing the soluble ectodomains of (i) human TREM2 fused to the Fc domain of human IgG4 (sTREM2-Fc), (ii) AD-associated TREM2 variants (sTREM2-R47HFc, sTREM2-R62H), (iii) mouse TREM2 (sTrem2-Fc) or (iv) Fc control was incubated with fA $\beta$ . These were spun at 18,000 g to pellet fA $\beta$  associated proteins. sTREM2, sTREM2-R47H and sTREM2-R62H were enriched in the fA $\beta$  pellet (Figs 1A and EV1A), whereas the Fc control was not detected in the pellet. Mouse sTrem2 also showed binding to A $\beta$  fibrils. Similar pull-down assay between fA $\beta$  and full-length TREM2 was conducted using the cleared RIPA lysate from TREM2, TREM2-R47H, and TREM2-R62H transiently transfected into HEK293T cells. Although less efficient, presumably because of detergent present in the lysate, full-length TREM2 and the AD variants were pulled down by fA $\beta$  (Figs 1B and EV1B).

Multiple studies show TREM2 ectodomain interacts with APOE (Atagi *et al*, 2015; Bailey *et al*, 2015; Yeh *et al*, 2016). To confirm that the sTREM2-Fc proteins are functional and bind APOE3, we co-transfected TREM2-Fc constructs with APOE3 and pulled down proteins that bound sTREM2-Fc with anti-IgG Fc agarose beads. These data show that the TREM2 ectodomain binds APOE and that there is no major difference in binding between the AD variants and WT TREM2 (Figs 1C and EV1C). In this experiment, a minor interaction between the human sIgG4-Fc domain and APOE3 is observed.

TREM2 is a member of a multiprotein family that is divergent between human and mice. We explored whether select members of

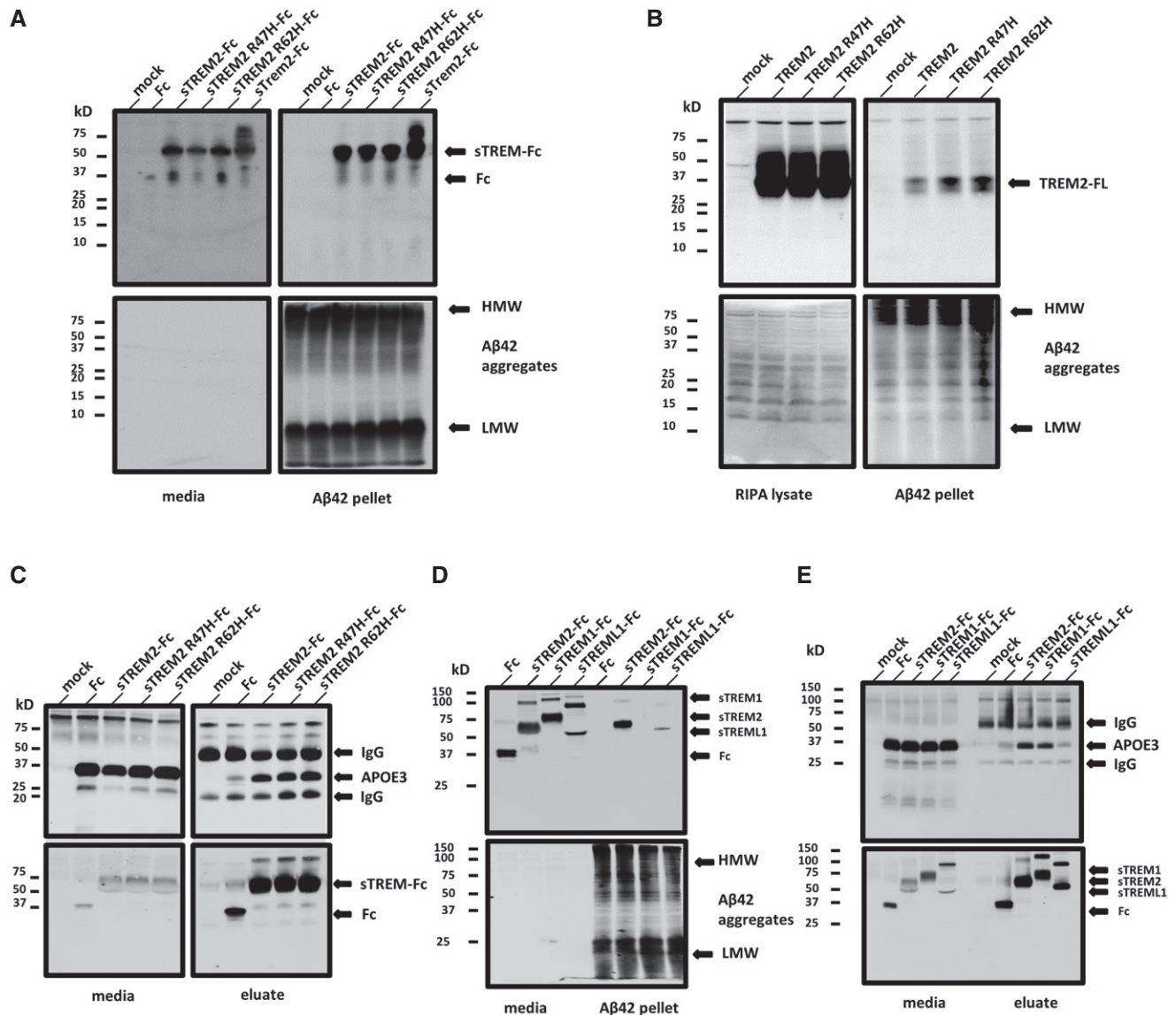


**Figure 1. Soluble TREM2 and soluble TREM1-Fc bind Aβ42 fibrils.**

**A** Media from soluble TREM2-Fc transfected HEK293T cells incubated with Aβ42 fibrils. Top left panel shows original media samples. Top right panel shows the presence of soluble TREM2 associated with Aβ42 pellet. The bottom two panels represent the same samples as the top, but probed with 6E10.

**B** RIPA lysate from TREM2 transfected HEK293T cells incubated with Aβ42 fibrils. Top left panel shows original RIPA lysate samples, and top right panel shows the presence of TREM2 associated with Aβ42 pellet. The bottom two panels represent the same samples as the top, but probed with 6E10.

**C** Media from soluble TREM2-Fc and APOE3 co-transfected HEK293T cells incubated with agarose beads anti-human IgG Fc. Left panels show original media samples. Right panels show the purified soluble TREM2-Fc (bottom) and the presence of APOE3 with the purified soluble TREM2-Fc (top).

**D** Media from soluble TREM-Fc family member transfected HEK293T cells incubated with Aβ42 fibrils. Top panel shows original media sample and the presence of TREM family members associated with Aβ42 pellet. Bottom panel shows original media and Aβ42 pellet probed with 6E10.

**E** Media from soluble TREM-Fc family members and APOE3 co-transfected HEK293T cells incubated with agarose beads anti-human IgG Fc. Top panel shows original media sample and the presence of soluble TREM family members associated with APOE3. Bottom panel shows original media and purified soluble TREM-Fc family members probed with anti-V5.

Data information: All experiments were replicated 3 independent times. Western blots in panels (A, B and C) have been cropped. The originals showing the supernatant fractions are available as Fig EV1.

Source data are available online for this figure.

the TREM2 family bind Aβ42 fibrils and APOE. We repeated the Aβ pull-down experiments in Fig 1A with two other soluble family members, which share low sequence homology with each and

other: TREM1-Fc and TREM1L1-Fc. In Fig 1D, we confirm presence of soluble TREM2-Fc and TREM1L1-Fc in the pelleted Aβ42 fibrils. Soluble TREM1-Fc was not detected in the pelleted Aβ42.

TREM1-Fc like soluble TREM2-Fc interacts with APOE3, but there is lack of detectable interaction between soluble TREM1-Fc and APOE3 (Fig 1E).

### Soluble TREM2-Fc and AD variants interact with A $\beta$ monomers or APOE with a similar affinity, and soluble TREM-Fc family members interact with A $\beta$ 42 oligomers with a higher affinity

We used BioLayer Interferometry (BLI) to further explore the interaction between A $\beta$  and TREM2 and other TREM family members. By immobilizing the TREM proteins on the BLI sensor, ligand interaction can be monitored in real time, enabling precise determination of the association and dissociation constants. As poorly soluble fA $\beta$  does not produce detectable binding in this assay even with high-affinity control anti-A $\beta$  antibodies, we were only able to assess binding with A $\beta$ 42 oligomers and A $\beta$ 40 and A $\beta$ 42 monomers. We initially explored interactions between A $\beta$ 42 oligomers and sTREM2-Fc in the BLI assay. These data revealed that sTREM2 bound A $\beta$ 42 oligomers with high affinity largely attributable to a very slow dissociation. In these initial studies, we also found no interaction between the Fc alone and A $\beta$ 42 oligomers. Further, when a high-affinity anti-A $\beta$ 1-16 antibody (Ab5) was incubated following the dissociation step, we were able to demonstrate that the A $\beta$  oligomers were indeed tightly complexed with sTREM2 on the sensor (Fig EV2A). After further optimization of the assay (see methods), we systematically evaluated the binding of sTREM-Fc proteins to various concentrations of A $\beta$ 42 oligomers, A $\beta$ 42 monomers A $\beta$ 40 monomers, as well as lipidated recombinant APOE3 and APOE4 (Figs 2A and B, and EV2B). Under these optimized conditions, no sFc binding is observed, and non-specific binding of APOE3 or APOE4 eliminated. These studies enabled precise determination of the  $K_{on}$ ,  $K_{dis}$  (Koff), and the overall KD (Fig 2C) of various form of A $\beta$  and APOE under identical conditions. These studies revealed very high-affinity binding between A $\beta$ 42 oligomers and sTREM2-Fc and the AD variants (<1.0 E-12 M). This strong binding is largely attributable to the apparent irreversibility of the binding. Indeed, the dissociation constants are the maximal measurable ( $K_{dis} = 1.0 \text{ E-}07 \text{ 1/s}$ ) on the Octet Red instrument. In contrast to the binding observed between sTREM2 and A $\beta$ 42 oligomers, binding to A $\beta$ 42 monomers was much weaker and reversible (KD from 1.4 to 2.9 E-07 M). The KDs of the WT TREM2 were not statistically different from the AD variants. Binding to A $\beta$ 40 monomers was similar to binding to A $\beta$ 42 monomers (KDs from 1.4 to 2.7 E-07 M), and again, the KDs of the WT TREM2 were not statistically different from the AD variants. We also established KDs in the nm range for binding of lipidated APOE3 and APOE4 with sTREM2. KDs for APOE3 binding sTREM2 or the AD variants were very similar and not statistically different. Binding of APOE4 revealed a slight increase in binding affinity of R47H variant (1.7 fold) and the R62H variant (1.56-fold) with APOE4 that was statistically significant. Given the irreversible nature of the A $\beta$ 42 oligomers binding to sTREM2, we explored whether the binding of A $\beta$ 42 oligomers could block interaction with APOE3. We evaluated whether pre-incubation with A $\beta$ 42 oligomers to sTREM2 could block subsequent interaction with APOE3. As shown in Fig 3, binding of A $\beta$ 42 oligomers blocked APOE3 binding. In contrast, addition of A $\beta$ 42 oligomers to sTREM2 previously bound to APOE3 did not block subsequent

interaction with A $\beta$ 42 oligomers. We next examined the binding of select soluble mouse and human TREM family members with A $\beta$ 42 oligomers by BLI (Fig 2D). TREM1 showed a similar high-affinity binding of A $\beta$ 42 oligomers to TREM2 but the interaction between TREM1 and A $\beta$ 42 oligomers was much weaker (1.1E-7 M). In contrast, both mouse Trem1 and Trem1l bound A $\beta$ 42 oligomers with high affinity.

We further investigated the binding of fA $\beta$  with soluble TREM2-Fc and the AD variants by an ELISA binding assay due to their unsuitability with BioLayer Interferometry. We compared the binding of fA $\beta$ , A $\beta$ 42 monomers, and A $\beta$ 42 oligomers with soluble TREM2-Fc and the AD variants. In Fig EV3, A $\beta$ 42 fibrils incubated with soluble TREM2-Fc and the AD variants or soluble Trem2-Fc increased weakly the signal compared to the Fc control and showed no significant differences. The A $\beta$ 42 oligomers incubated with soluble TREM2-Fc or the AD variants or soluble Trem2-Fc produced a signal significantly higher compared to Fc control and around two times stronger than the one from the A $\beta$ 42 monomers. In Fig 4A, we tested A $\beta$ 42 monomers at higher concentrations. A significant signal between Fc control and the soluble TREM2-Fc or the AD variants or soluble Trem2-Fc is obtained at 1,000 nM A $\beta$ 42 monomers and more. This result confirms the binding of A $\beta$ 42 monomers with soluble TREM2 and the AD variants and soluble Trem2-Fc without significant differences between all of them. We then repeated a similar ELISA assay with soluble TREM-Fc family members and A $\beta$ 42 oligomers. In Fig 4B, only soluble TREM2-Fc and soluble TREM1-Fc produced a significant signal compared to Fc control. This result confirms the binding of A $\beta$ 42 oligomers with soluble TREM2-Fc and soluble TREM1-Fc and lack of binding with soluble TREM1-Fc.

Collectively, these biochemical experiments confirm a direct interaction between A $\beta$ 42 and TREM2 and the AD variants TREM2 R47H or TREM2 R62H and Trem2 without any significant differences. A $\beta$ 42 oligomers have a stronger affinity for TREM2 than A $\beta$ 42 monomers. TREM1 also binds A $\beta$ 42 oligomers, but failed to bind APOE3 contrary to TREM2 or TREM1.

### Expression of TREM2 activates NFAT signaling and increases internalized A $\beta$ 42

We investigated whether the binding of A $\beta$ 42 oligomers with TREM2 activates cell signaling by exposing 2B4 NFAT-GFP reporter cells transduced with TREM2 to various concentrations of A $\beta$ 42 oligomers. As other TREM2 ligands activate NFAT in these cells, we predicted that the high-affinity interaction with A $\beta$ 42 oligomers would also induce NFAT signaling. Control cells exposed to A $\beta$ 42 oligomers weakly activated the GFP reporter compared to WT TREM2 expressing cells (Fig 5A). Cells expressing TREM2 R47H and exposed to A $\beta$ 42 oligomers also activated the GFP reporter, but at each concentration, the signal was lower than the signal in WT TREM2 transduced cells. Further study of reporter cells expressing WT TREM2, TREM2 R47H TREM2 R62H, or a putatively frontotemporal dementia (FTD) variant (TREM2 T96K) shows that the TREM2 AD variants R47H and R62H reduced NFAT activation whereas the FTD variants TREM2 T96K activated NFAT signaling at similar level than TREM2 (Fig 5B). These data demonstrate that TREM2 activates NFAT signaling in presence A $\beta$ 42 oligomers and this activation is reduced by the AD variants TREM2 R47H or R62H.

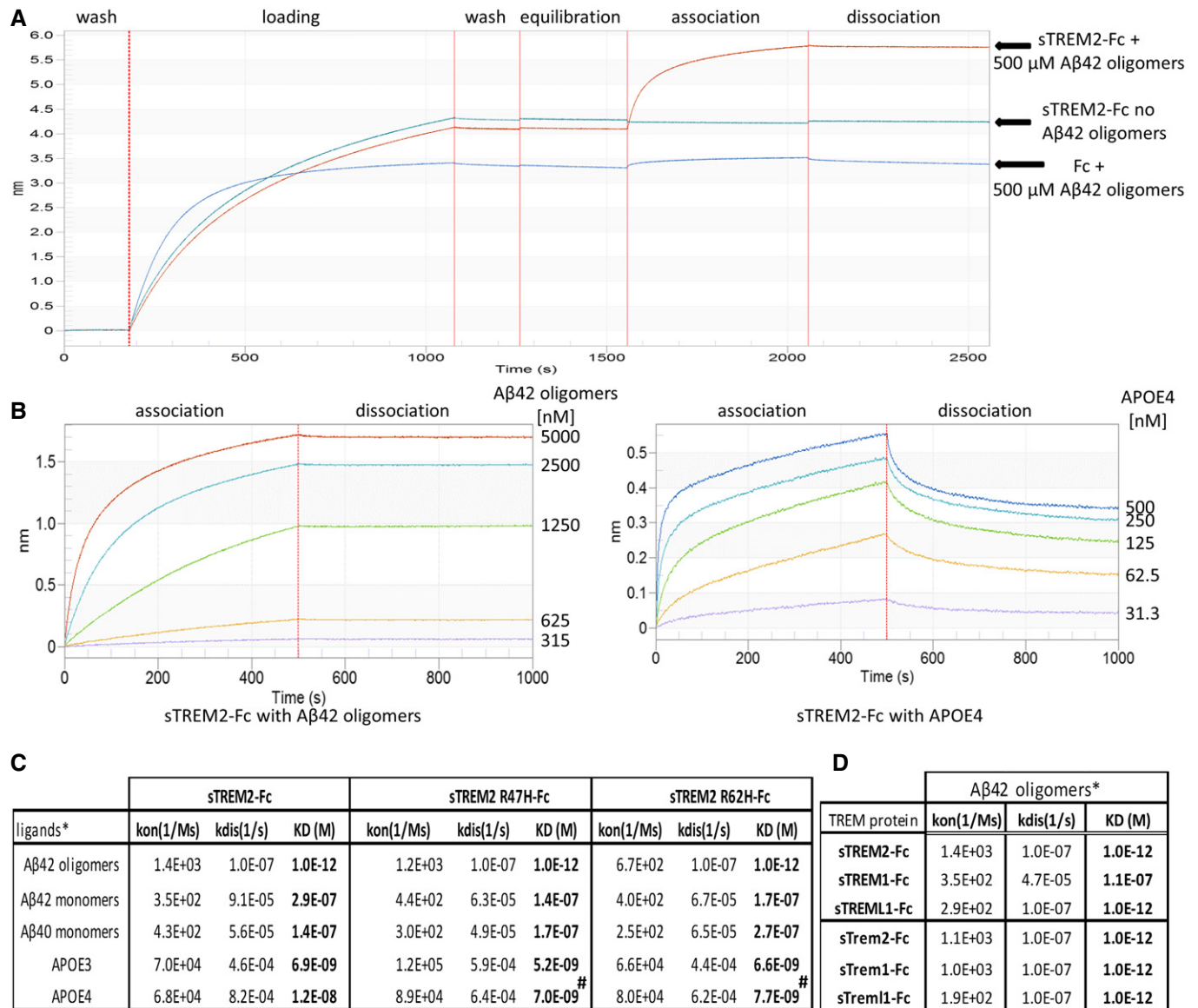


**Figure 2. Binding affinity of soluble TREM-Fc family members and AD variants with Aβ42 oligomers, Aβ42 monomers, Aβ40 monomers, and APOE3 and APOE4.**

BioLayer Interferometry experiments were performed to measure ligand binding affinity with soluble TREM-Fc family members and mouse soluble TREM-Fc family members.

A Schematic representation of a full-length experiment.

B Schematic representation of Aβ42 oligomers (right panel) and APOE4 (left panel) binding with soluble TREM2-Fc at various concentrations. Curves were fit by setting buffer control (no ligand) to  $y = 0$ .

C Calculated Kon, Kdis, and KD values for Aβ42 oligomers or Aβ42 monomers, Aβ40 monomers, or APOE3 or APOE4 association/dissociation with soluble TREM2-Fc and AD variants. Kinetic constants were calculated using five different concentrations of ligand, and the entire experiment (including new ligand preparations and purifications of soluble TREM-Fc) was repeated twice ( $^{*}P < 0.05$ , ANOVA, Tukey's multiple comparison test, see Appendix Table S1 for exact P-value).

D Calculated Kon, Kdis, and KD value for Aβ42 oligomers association/dissociation with soluble human vs. mouse TREM-Fc family members. Kinetic constants were calculated using five different concentrations of ligand, and the entire experiment (including new ligand preparations and purifications of soluble TREM-Fc) was repeated twice.

Data information: Kon; constant of association, Kdis; constant of dissociation, KD; equilibrium constant of dissociation.

TREM2 expression in non-phagocytic cells confers phagocytic activity (Hsieh et al, 2009). To evaluate whether TREM2 expression induces Aβ42 uptake, we incubated Aβ42 over HEK293T cells transiently transfected with TREM2 and quantified internalized Aβ42. Compared to

control transfection, TREM2 expression increased the amount of internalized Aβ42 (Fig 5C). TREM2 R47H and R62H also increased internalization levels relative to control, but the amount internalized was significantly less than that observed with WT TREM2 (Fig 5C).

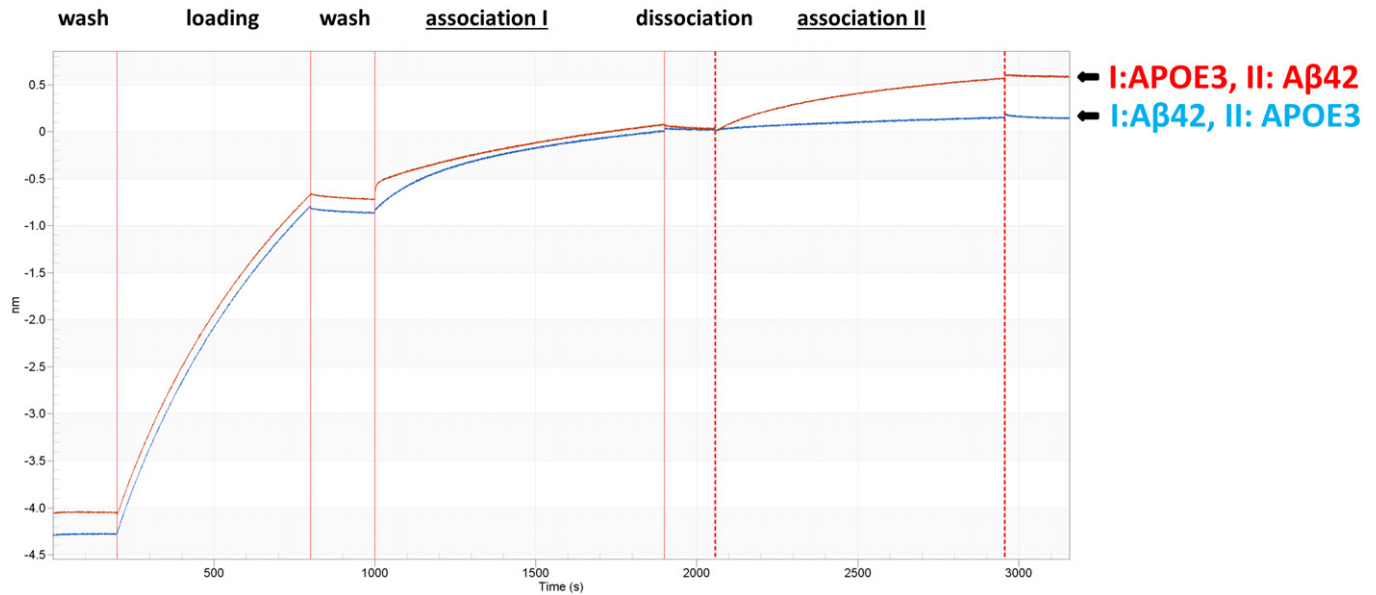


**Figure 3. Binding of Aβ42 oligomers on soluble TREM-Fc prevents binding of APOE3 in BiLayer Interferometry.**

BiLayer Interferometry experiments were performed to evaluate the binding capacity of APOE3 on soluble TREM2-Fc pre-incubated with Aβ42 oligomers. Schematic representations of two sequential associations of ligand on soluble TREM2-Fc are represented by I and II. Soluble TREM2-Fc loaded on a sensor is first incubated with APOE3 (association I) followed by a second incubation with Aβ42 oligomers (association II) or the reverse-incubated with Aβ42 oligomers (association I) followed by a second incubation with APOE3 (association II). All experiments were replicated 3 independent times.

We conducted several studies to further explore the reduced uptake observed by the AD variants. First, we investigated whether the shedding of TREM2 is affected by Aβ. If Aβ binding induces shedding of the TREM2 ectodomain and the AD variants are shed more, this could explain the decreased uptake observed. However, as observed in Fig 5D, despite similar levels of membrane-associated TREM2, TREM2 R47H, and TREM2 R62H, the amount of soluble TREM2 was similar and not altered by oligomeric Aβ. We also rigorously evaluated cell-surface levels of TREM2 using cell-surface biotinylation studies. These studies (Fig 5E) again revealed no significant differences in levels as previously observed (Kleinberger *et al*, 2014; Kober *et al*, 2016).

## Discussion

We find that TREM2 binds to various forms of Aβ with a very high-affinity interaction with Aβ42 oligomers. Further, TREM2 appears capable of mediating Aβ internalization and Aβ oligomers induce NFAT signaling through TREM2. These data establish a direct link between Aβ aggregates, which are implicated as initiators of the pathological cascade in AD and TREM2 a microglial immune receptor. No difference in binding affinity between the AD-associated variants and WT TREM2 to any form of Aβ is detected. However, AD-associated TREM2 variants appear to reduce both Aβ internalization and downstream NFAT signaling. Consistent with other published data, these data indicate that TREM2 variants associated with AD risk may act through subtle loss of function (Song *et al*, 2018). These data are also consistent with the reported protection from AD attributable to a non-coding nucleotide polymorphism in

the TREM locus that increases both TREM2 and TREM1 expression (Carrasquillo *et al*, 2017). Indeed, a recent modeling study showed that increased TREM2 levels reduced amyloid levels in an APP mouse model and attenuated a number of other amyloid-associated phenotypes in this model (Lee *et al*, 2018). As cell-surface levels of the AD variants and WT TREM2 are similar in these studies and there is no detectable difference in internalization or processing either in the presence or absence of Aβ, additional studies will be needed to better understand the functional differences between the AD variants and WT TREM2, which our data strongly suggest are downstream of the initial binding event.

The differential binding affinities between various forms of Aβ and TREM2 are interesting. Binding to monomeric Aβ is relatively weak, whereas binding to oligomers is essentially irreversible. Indeed, prior interaction of Aβ oligomers blocks binding of a second ligand, lipidated APOE. We have been unable to directly assess affinities to fAβ by BLI due to technical reasons, but do observe strong interaction in the fAβ pull-down assay in the absence of detergent. In the presence of detergent or by ELISA, which also contains small amount of detergent in the binding buffer, we observe a weaker interaction. Collectively these data support a model in which various forms of Aβ interact with TREM2 with different affinity and that difference in affinity appears to be attributable to conformational differences.

Given (i) the polarized localization of TREM2 on the microglial cells surrounding amyloid plaques (Jiang *et al*, 2014; Yuan *et al*, 2016; Jay *et al*, 2017) and (ii) the lack of homing of microglial to plaques that is observed in knockout mouse models (Ulrich *et al*, 2014; Jay *et al*, 2015, 2017; Wang *et al*, 2015, 2016; Yuan *et al*, 2016), it is intriguing to consider that high-affinity interaction



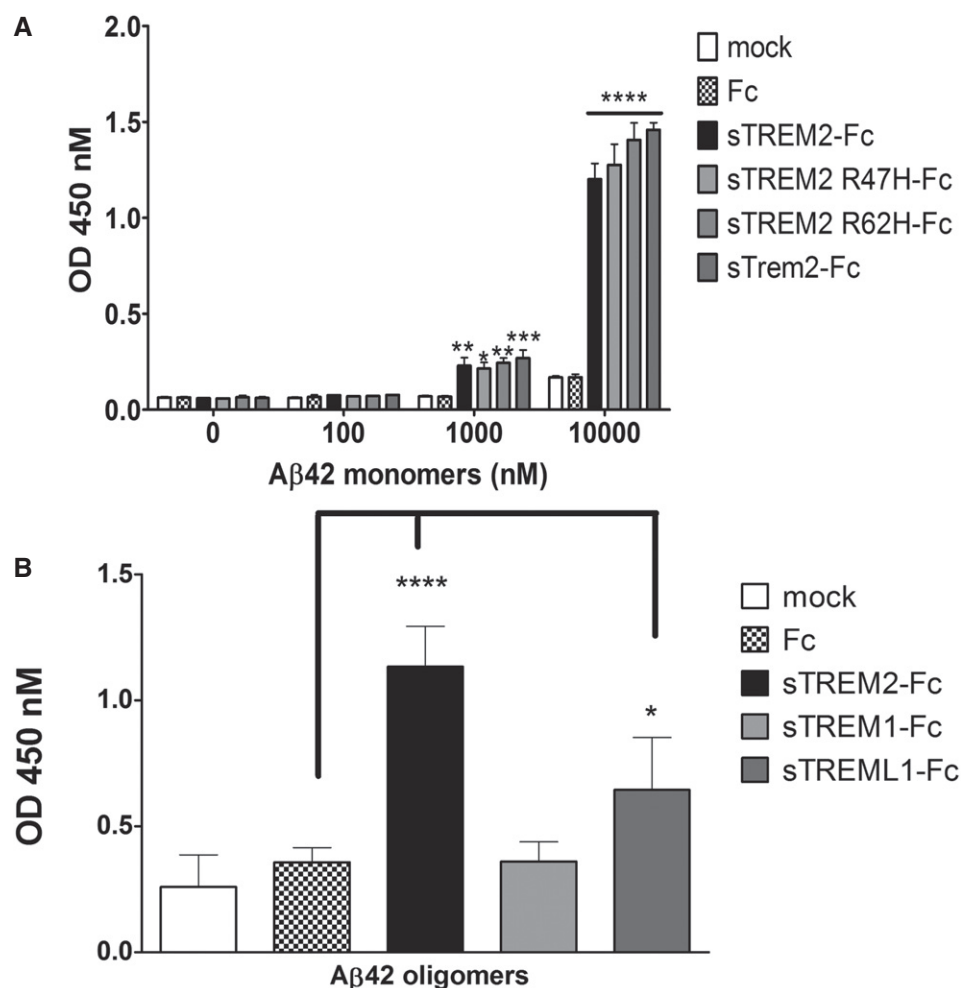


**Figure 4. Binding of Aβ42 monomers and Aβ42 oligomers with soluble TREM2-Fc measured by ELISA assay.**

ELISA plates were coated with purified soluble TREM2-Fc and then incubated with various concentrations of Aβ42 monomers or 1 μM Aβ42 oligomers.

A Binding of Aβ42 monomers with soluble TREM2-Fc shows a dose-dependent signal. Results were expressed as the OD450 averaged ± standard error ( $n = 3$ ; \* $P < 0.05$ , \*\* $P < 0.01$ , \*\*\* $P < 0.001$ , \*\*\*\* $P < 0.0001$ , two-way ANOVA, Bonferroni multiple comparisons, see Appendix Table S2 for exact  $P$ -values).

B Binding of 1 μM Aβ42 oligomers with soluble TREM-Fc family members. Results were expressed as the OD450 averaged ± standard error ( $n = 4$ , \* $P < 0.05$ , \*\*\*\* $P < 0.0001$ , ANOVA, Bonferroni multiple comparisons, see Appendix Table S2 for exact  $P$ -values).

between Aβ aggregates and TREM2 could underlie these observations. Although Aβ oligomers are described as soluble, immunohistochemical studies with select anti-oligomeric antibodies suggest that Aβ in an oligomeric conformation is present within plaques (Koffie *et al*, 2009). This raises an interesting speculation that TREM2 could interact with this plaque-associated oligomeric conformer of Aβ resulting in cell-surface polarization and microglial homing (Tanzi, 2015; Yeh *et al*, 2017). Given the promiscuous ligand specificity of TREM, and the apparent ability of Aβ oligomers to block subsequent ligand binding, it is hard to predict what the biological effects of engagement of TREM2 by Aβ oligomers would be in the peri-plaque region. Depending on relative concentration of ligands and relative efficiency of ligand-induced signaling the net result could be either prolonged TREM2 activation or reduced TREM2 activation.

Human TREM2 and mouse Trem2 are 68% identical and 76% homologous, and they bind Aβ oligomers with similar affinity.

These data would suggest that genetic manipulations of mouse Trem2 are likely to be informative with respect to the interactions with Aβ. Although TREM2 is the most abundant TREM family member based on expression levels in the brain, TREML1 is present at appreciable levels (Carrasquillo *et al*, 2017). Further, mouse Trem1 expression in the brain is dramatically increased by the transgene inserted to knockout TREM2 in one of the TREM2 mouse knockout models (Kang *et al*, 2018). Given that Trem1 shows strong interaction with Aβ oligomers, this could contribute to the discrepancies reported in the various knockout models with respect to effects on amyloid deposition. Our studies of human TREM1 and TREML1 show that TREML1 binds Aβ oligomers with high affinity but TREM1 does not. Conversely, TREM1 binds lipidated APOE but TREML1 does not. In contrast, both mouse Trem1 and Trem1 bind Aβ oligomers. These data can provide a basis for understanding both the larger biological role of TREM2 and family members in AD but also provide a

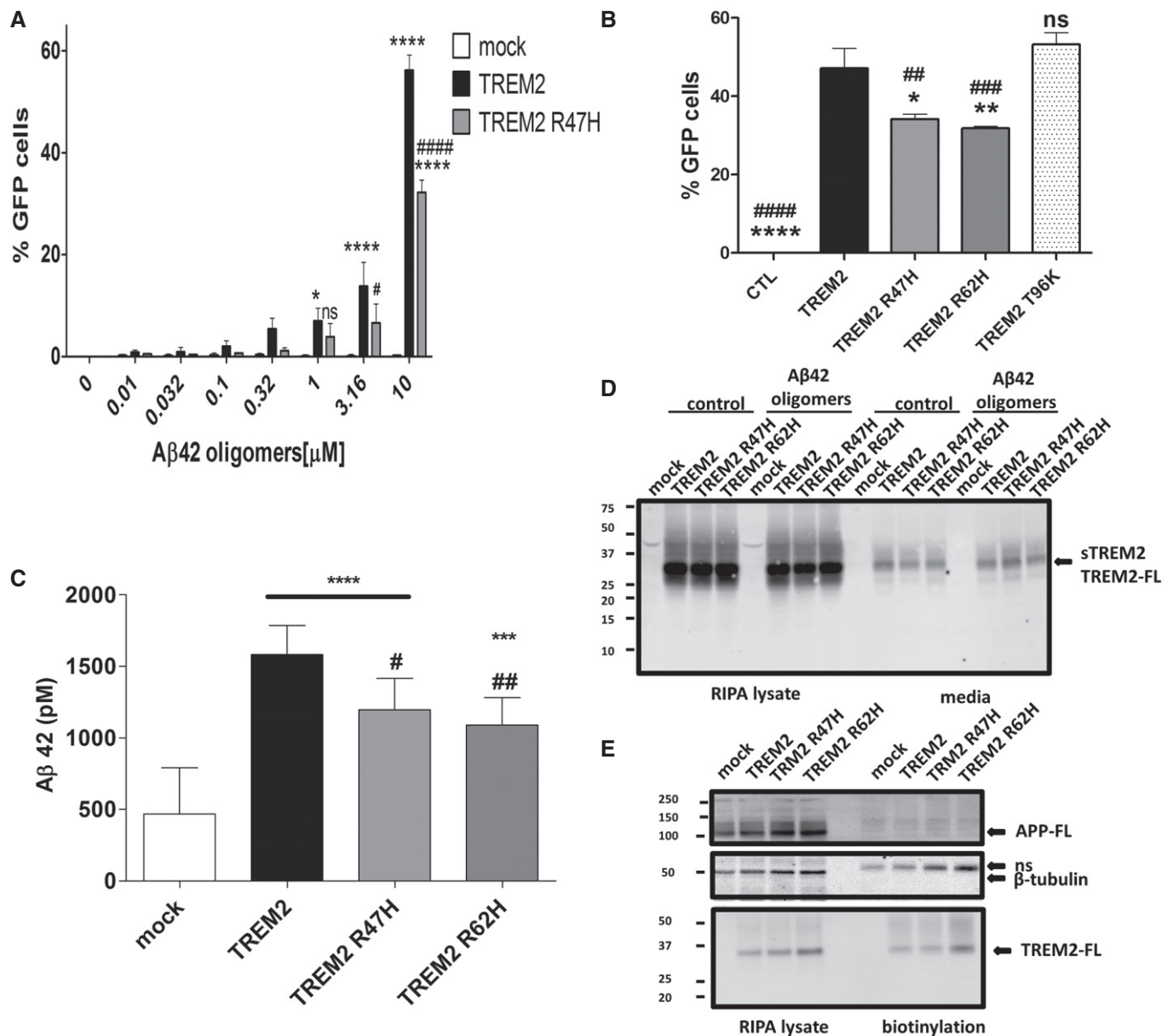


**Figure 5. Aβ42 oligomers induce TREM2 signaling and TREM2 mediates increased uptake of Aβ42 in HEK cells.**

- A** 2B4 NFAT-GFP reporter cells transduced with TREM2 or AD variant R47H were incubated with various concentrations of Aβ42 oligomers for 12 h. GFP expression was detected at 1 μM Aβ42 oligomers with TREM2 transduced cells. No GFP expression was detected with Aβ42 oligomers from control transduced cells. Results were expressed as the percentage GFP cells averaged ± standard error ( $n = 3$ ,  $*P < 0.05$  compared with mock,  $****P < 0.0001$  compared with mock,  $^{\#}P < 0.05$  compared with TREM2,  $****P < 0.0001$  compared with TREM2, two-way ANOVA, Bonferroni multiple comparisons, see Appendix Table S3 for exact  $P$ -values).
- B** B-2B4 NFAT-GFP reporter cells transduced with TREM2 or variants (R47H, R62H, and T96K) were incubated with 10 μM Aβ42 oligomers for 12 h. No GFP expression was detected with Aβ42 oligomers from control transduced cells. Results were expressed as the percentage GFP cells averaged ± standard error ( $n = 3$ ,  $*P < 0.05$  compared with TREM2,  $**P < 0.05$  compared with TREM2,  $****P < 0.0001$  compared with TREM2,  $^{\#}P < 0.01$  compared with TREM2 T96K,  $****P < 0.0001$  compared with TREM2,  $****P < 0.0001$  compared with TREM2,  $^{\#}P < 0.01$  compared with TREM2 T96K,  $****P < 0.0001$  compared with TREM2, ANOVA, Dunnett's multiple comparisons test, see Appendix Table S3 for exact  $P$ -values).
- C** HEK293T cells transfected with TREM2 or AD variant incubated with 500 nM Aβ42 monomers were lysed for Aβ42 quantifications by ELISA. Expression of TREM2 increases Aβ42 level detected compared to mock control as well the AD variant. Results were averaged ± standard error ( $n = 9$ ,  $^{\#}P < 0.05$  compared with TREM2,  $****P < 0.0001$  compared with TREM2,  $****P < 0.0001$  compared with mock,  $****P < 0.0001$  compared with mock, ANOVA, Tukey's multiple comparison test, see Appendix Table S3 for exact  $P$ -values).
- D** HEK293T cells transfected with TREM2 were incubated with Aβ42 oligomers for 16 h. Conditioned media and cell lysate were analyzed by Western blot for TREM2 (RIPA lysate) and soluble TREM2 (media) detection. Experiment was replicated 3 independent times.
- E** HEK293T cells transfected with TREM2 were subjected to cell membrane biotinylation for purification. Bottom panel in (D) shows the presence of TREM2 in the purified product. Endogenous APP and β-tubulin were used as controls for the purification (middle and upper panels). Experiment was replicated 3 independent times.

Source data are available online for this figure.

framework to understand the structural features of the various TREM molecules required for A $\beta$  interaction.

We confirmed the previously reported binding between TREM2 and APOE, although some of the details that we report regarding binding are distinct (Atagi *et al*, 2015; Bailey *et al*, 2015; Yeh *et al*, 2016). Whereas other groups have reported reduced binding of APOE with TREM2 AD variants (Atagi *et al*, 2015; Bailey *et al*, 2015; Yeh *et al*, 2016), we find little difference between the binding affinity between lipidated APOE and TREM2 or the AD variants. In fact, for APOE4 binding, we see slightly increased in affinity for the AD variants compared to WT TREM2. Though statistically significant, this is relatively small difference and unlikely to translate into biological differences with respect to function. Differences between our data and previous reports may be due to technical differences. Yeh *et al* (2016) make claims about binding affinity based on BLI but did not actually measure association and dissociation constants. Yuka *et al* evaluated binding of TREM2/APOE by dot blot and ELISA assays, which again do not provide precise data on kinetics of binding, and Bailey *et al* reported that TREM2 R47H reduced the affinity of TREM2 for APOE used ELISA assay (Atagi *et al*, 2015; Bailey *et al*, 2015). In contrast to Yuka *et al*, who reported a lack of interaction between TREM1 and APOE in dot blot assay, we detect an interaction between secreted TREM1 and APOE3 from media. (Atagi *et al*, 2015).

An interaction between TREM2 and A $\beta$ 42 oligomers has also recently been reported by several other groups (Zhao *et al*, 2018; Zhong *et al*, 2018). Our data and these reports consistently show stronger binding between TREM2 and A $\beta$  oligomers compared to monomers (Zhao *et al*, 2018). In contrast to these other studies, we do find reproducible and appreciable binding between monomeric A $\beta$  and TREM2, though the interaction is weaker than the interaction with a known ligand APOE and much weaker than the interaction with oligomeric A $\beta$ . We also observe a much higher binding affinity between oligomeric A $\beta$  and TREM2 than what is reported in these other studies. In our studies, this high affinity is primarily driven by a Kdis that is the lowest measurable on the Octet instrument. A prediction of the extremely low Kdis is that the nearly irreversible binding of oligomeric A $\beta$  to TREM2 would block interaction with another ligand. We tested this prediction with APOE and find that this is indeed the case—prior incubation of A $\beta$  oligomers with TREM2 blocked subsequent binding of APOE to TREM2. A final and important discrepancy between these reports is that we reproducibly do not detect differences in affinity between various forms of A $\beta$  and TREM2 WT and the AD variants in either the BLI studies or in ELISA assays. Notably, although these other reports use BLI to calculate affinity of TREM2 WT to oligomeric A $\beta$ , only solid-phase plate binding assays are used to show differences in the affinity between A $\beta$ 42 oligomers and TREM2 or the TREM2 variants (Zhao *et al*, 2018; Zhong *et al*, 2018). Clearly, many factors ranging from binding buffers to protein purity and also form A $\beta$  oligomers can alter affinity measurements. It is likely that such differences may account for the quantitative differences in binding affinity observed in our study compare to these other studies. Additional studies will be needed to reconcile these differences, which may have important pathophysiologic implications. Indeed, we show consistent effects of AD variants on both A $\beta$  internalization and

NFAT signaling both consistent with a partial loss of function. However, our data indicate that these functional effects are not attributable to decreased affinity for A $\beta$  under the conditions tested. The functionality of interaction between A $\beta$  oligomers and TREM2 showed an activation of NFAT signaling as observed by Zhong *et al* (2018). This signaling activation was indirectly confirmed by showing that A $\beta$ 42 oligomers enhanced the interaction between TREM2 and DAP12 and induced SYK phosphorylation, an important factor for NFAT signaling (Zhao *et al*, 2018).

Reports exploring TREM2 deficiency in mouse models of A $\beta$  deposition have shown both differing effects on A $\beta$  levels during early and late stages and in some cases no change in overall amyloid loads (Ulrich *et al*, 2014; Jay *et al*, 2015, 2017; Wang *et al*, 2015, 2016). Studies that showed effects on A $\beta$  deposition reported changes in A $\beta$  loads were rather modest and regional in nature (Ulrich *et al*, 2014; Wang *et al*, 2016). This suggests that any interaction between TREM2 and A $\beta$  (or perhaps even co-deposited APOE) in the peri-plaque region alters microglial response to the plaque with a minimal effect on plaque clearance (Jiang *et al*, 2014; Jay *et al*, 2015, 2017; Wang *et al*, 2015; Yuan *et al*, 2016). Given this modeling data, we would suggest that any interaction between TREM2 and A $\beta$  (or perhaps even co-deposited APOE) in the peri-plaque region alters microglial response to the plaque but would have minimal effect on plaque clearance. Notably, recent data from one of our group show that R47H TREM2 variant fails to restore microglial homing and activation around amyloid plaques in the mouse knockout background (Song *et al*, 2018). They also found that sTREM2-R47H despite being present at equal levels as a common variant (CV) of sTREM2 was not associated with plaques or neurons, whereas the sTREM2-CV was. Another group showed that AD mice Trem2 R47H heterozygous reduced myeloid cell responses to amyloid deposition and reduction in proliferation and CD45 expression around plaque (Cheng-Hathaway *et al*, 2018). These data present a conundrum given that we showed kinetics of binding of the R47H and WT TREM2 to A $\beta$  are indistinguishable. Further, they are hard to reconcile functionally with the increased shedding of the Han Chinese TREM2 variant that is reported to increase ectodomain shedding, but would not be expected to alter the functionality of the ectodomain (Schlepckow *et al*, 2017; Thornton *et al*, 2017). The overexpression of TREM2 appears protective. Previous studies showed protective functions of TREM2 overexpression by facilitating A $\beta$ 42 phagocytosis and inhibited proinflammatory responses in cultured primary microglia, reducing AD-related neuropathology in mice APP<sup>swE</sup>/PS1<sup>dE9</sup> and ameliorating tau pathology a tau mice model (Jiang *et al*, 2014, 2016b). Our results tend in the same direction by showing benefits of TREM2 expression like increasing A $\beta$ 42 phagocytosis and activating cell signaling.

We present biochemical and cellular data that demonstrate that TREM2 and select family members can bind to various forms of A $\beta$  with the highest affinity interaction observed for A $\beta$  oligomers, and we confirm an interaction between TREM2 and APOE (Atagi *et al*, 2015; Bailey *et al*, 2015; Yeh *et al*, 2016). Intracellular signaling elicited following binding by A $\beta$  oligomers is attenuated by AD-associated TREM2 variants, though the AD variants appear to bind both A $\beta$  and lipidated APOE with similar affinity to interaction with WT TREM2. These data link TREM2 to physical interactions with two

key molecules in Alzheimer's disease and provide clues that can illuminate the clearly complex biology of TREM2 in health and disease.

## Materials and Methods

HEK293T cells were grown in DMEM supplemented with Hyclone 10% fetal bovine serum (GE, Utah, USA) and 1% penicillin/streptomycin (Life Technologies, NY, USA). Cells were transiently transfected with calcium phosphate. 2B4 reporter cells were maintained in RPMI (Sigma, MO, USA) supplemented with 10% FBS, 1% GlutaMAX (Gibco, NY, USA), 1 mM sodium pyruvate (Corning, VA, USA), 1% penicillin/streptomycin (Gibco, NY, USA), and transfected by retroviral transduction.

### Antibodies

Antibodies are listed in Table 1.

### cDNA constructions

pcDNA5-FRT-TO-TREM2, pcDNA5-FRT-TO-TREM2 R47H, pcDNA5-FRT-TO-TREM2 R62H were a gift from Christian Haass (Kleinberger *et al*, 2014). Soluble domains of human TREM2, TREM1, TREML1 and mouse Trem2, Trem1, and Trem1l were cloned in frame with human IgG Fc4 and V5 epitope in pTR2-CBA plasmid (GeneScript, NJ, USA). TREMs cDNA constructions are listed in Table 2.

### A $\beta$ 42 fibrils pull down

A $\beta$ 42 fibril preparation and pull-down assay were performed as described (Chakrabarty *et al*, 2015; Pinotsi *et al*, 2016). Conditioned media with 5 mM EDTA or cellular lysate (RIPA SDS containing buffer) were centrifuged at 18,000 g for 5 min at 4°C to remove insoluble materials. Supernatants were incubated with A $\beta$ 42 fibrils for 1 h at room temperature. A $\beta$ 42 fibrils were centrifuged at 18,000 g for 5 min at 4°C to pellet the fibrils. Fibrils were washed with RIPA buffer or PBS (for conditioned media samples) and centrifuged again. The pelleted A $\beta$ 42 fibrils were then dissolved in protein loading buffer (31.25 mM Tris-HCl pH 7.5, 2% LDS, 10% glycerol, 1.5%  $\beta$ -mercaptoethanol, and Orange G). Cell conditioned media samples or cell lysates were also incubated with the fibril assay buffer to verify proteins aggregations. Dissolved fibrils were heated at 95°C for 5 min and loaded on Bis-Tris precast gels (Bio-Rad, CA, USA) and transferred on PVDF membrane for Western blotting. TREM2 was detected with HA antibody, soluble trem2-Fc-V5 were detected with V5 antibody, and fibrils were detected with 6E10 antibody.

### Western blotting

PVDF membranes were blocked in TBS 0.5% casein a 1 h at room temperature. Primary antibody diluted in TBS with 0.2% Tween-20 (TBS-T) was incubated on the membrane 1 h at room temperature. The membranes were washed three times 5 min with TBS-T. Secondary antibodies were diluted in TBS-T and incubated 1 h at room temperature. The membranes were washed 3 times 5 min

**Table 1. List of antibodies used for Western blot and ELISA.**

Antibodies	Source	Usage, dilution
TREM2 CTF	Cell Signaling	Western blot, 1/2,500
HA tag	Cell Signaling	Western blot, 1/2,500
V5 tag	Invitrogen	Western blot, 1/5,000
Ab947 (APOE)	Chemicon	Western blot, 1/2,500
HRP-Anti-Human IgG Fc $\gamma$	Jackson ImmunoResearch Inc	ELISA (for detection), 1/2,000
2.1.3 (A $\beta$ 42)	Todd. E. Golde	ELISA (for coating), 50 $\mu$ g/ml
HRP-4G8	BioLegend	ELISA (for detection), 1/2,000
IRDye 800CW	LI-COR	Western blot (for detection), 1/12,500
Alexa Fluor 680 goat or rabbit	Invitrogen	Western blot (for detection), 1/25,000
6E10 (amyloid)	BioLegend	Western blot, 1/1,000

with TBS-T and then analyzed with Odyssey infrared imaging system (LI-COR Inc., NE, USA).

### Purification of secreted soluble TREM-Fc-V5 family members from cell conditioned media

Conditioned media from HEK293T-transfected cells was centrifuged 5 min at 800 g to clear cells and then transferred to a tube with 0.5% Triton X-100, complete protease inhibitors, and 5 mM EDTA. Samples were incubated 2 h at room temperature with anti-human IgG Fc-specific agarose beads (Sigma, MO, USA) and washed three times with PBS. Purified proteins from agarose beads were washed in PBS and eluted with 100 mM glycine pH 2.7 followed a neutralization (pH~7.5) with 1 M Tris-HCl pH 8.8. Alternatively, agarose beads were pre-blocked with 5% bovine serum albumin (Sigma, MO, USA) 2 h at room temperature and washed with PBS before the purification. Purified samples were verified by Western blot to confirm protein purification.

### APOE interaction assay

HEK293T cells were co-transfected with soluble TREM2-Fc family members and APOE3. The soluble TREM-Fc family members were purified as described above with BSA pre-blocked agarose beads anti-human IgG Fc specific. Agarose beads were washed with PBS 0.5% Triton and eluted with protein loading buffer. Eluates were loaded on Bis-Tris precast gels and transferred on PVDF membrane for Western blotting. Soluble TREM2 Fc-V5 and AD variants were detected with V5 antibody, and APOE3 was detected with Ab947 antibody.

### BioLayer interferometry

Soluble TREM2-Fc-V5 and TREM2-Fc-V5 family proteins were purified as described above with anti-human IgG Fc-specific agarose beads. A $\beta$ 42 monomers and oligomers were prepared as described (Stine *et al*, 2003). Kinetic determination of TREM2/A $\beta$ 42 oligomer was initially performed on the Octet RED384 instrument (ForteBio

**Table 2. List of TREMs cDNA constructs used for the experiments.**

Plasmid	Species	Notes	Epitope	Usage
sTREM2-Fc	Human	Soluble ectodomain	V5	Figs 1A, C, D, and E, 2, 3, and 4
sTREM2-R47H-Fc	Human	Soluble ectodomain AD variant	V5	Figs 1A and C, 2C, and 4
sTREM2-R62H-Fc	Human	Soluble ectodomain AD variant	V5	Figs 1A and C, 2C, and 4
sTREM1-Fc	Human	Soluble ectodomain	V5	Figs 1D and E, 2D, and 4B
sTREM1-Fc	Human	Soluble ectodomain	V5	Figs 1D and E, 2D, and 4B
sTrem2-Fc	Mouse	Soluble ectodomain	V5	Figs 1A, 2D, and 4A
sTrem1-Fc	Mouse	Soluble ectodomain	V5	Fig 2D
sTrem1-Fc	Mouse	Soluble ectodomain	V5	Fig 2D
TREM2	Human	Full-length protein	HA and FLAG	Figs 1B and 5C–E
TREM2-R47H	Human	Full-length protein AD variant	HA and FLAG	Figs 1B and 5C–E
TREM2-R62H	Human	Full-length protein AD variant	HA and FLAG	Figs 1B and 5C–E
TREM2-IRES-DAP12 TREM2-R47H-IRES-DAP12	Human	Full-length protein	No epitope	Fig 5A and B
TREM2 R62H-IRES-DAP12 TREM2 T96K-IRES-DAP12	Human	Full-length protein	No epitope	Fig 5B

(Pall), CA, USA), using anti-human Fc-specific sensors (AHC, ForteBio (Pall), CA, USA), PBS 0.002%, and Tween-20 as assay buffer. Briefly, measurements were performed at 30°C and sensors were activated in a 96-well microplate in PBS and agitated at 1,000 rpm for 10 min. Various dilutions of A $\beta$ 42 or human lipidated APOE3 and APOE4 (gift from Dr. David M. Holtzman) were loaded in a 384-well microtiter plate.

A second BLI assay was developed for compatibility APOE proteins utilizing Protein A sensors (ProA, ForteBio (Pall), CA, USA). Protein A sensors were loaded to near-saturation with soluble TREM-Fc-V5 family proteins in PBS, transferred to fresh PBS for baseline measurement, then associated with A $\beta$ 42 oligomer, human lipidated APOE3 or APOE4 ligands along a serial dilution. The sensors were finally moved back to PBS for disassociation. Constant of association (kon), constant of dissociation (kdis), and equilibrium constant of dissociation (KD) values were determined by global fitting of the binding curves for each ligands dilutions and calculated by applying a 1:1 interaction model (fitting local, full) using the ForteBio Data Analysis software (CA, USA) version 9.0.0.14.

### ELISA binding assay

Soluble TREM-Fc family member proteins were purified and eluted as previously described for the BioLayer Interferometry. Purified samples were coated overnight at 4°C in 96-well plates (Immulon 4HBX, Thermo Scientific, NY, USA) in 100 mM NaCO<sub>3</sub> pH 11. Plates washed with PBS twice and then blocked 3 h at room temperature with blocking buffer (Block Ace, Abd Serotec, Japan). Blocked samples were incubated with A $\beta$ 42 monomers, A $\beta$ 42 oligomers, or A $\beta$ 42 fibrils at specified concentration for 1 h at room temperature. A $\beta$  was detected with 4G8-HRP, and soluble TREM-Fc samples were detected with anti-human IgG HRP to insure similar coating level of proteins. Samples were developed with TMB substrate (KPL, Maryland, USA), and the reaction was stopped by adding 6.67% O-phosphoric acid (85%). The signal produced by HRP and TMB substrate was quantified by measuring the absorbance at 450 nm.

### A $\beta$ cellular uptake

HEK293T transfected cells from a 6-well plate were incubated 3 h with 500 nM A $\beta$ 42 monomers. Cells were washed two times with PBS, incubated with trypsin 5 min, and centrifuged 3 min at 500 g. Supernatant was removed, and cells were washed three times with a large volume of PBS (10–15 ml/wash). Pelleted cells were lysed with 100  $\mu$ l SDS 2% for 5 min, and then, 200  $\mu$ l of PBS was added. Samples were sonicated and centrifuged at 18,000 g for 15 min at 4°C. Samples were diluted 1/40 in EC buffer (PBS containing 0.1 mM EDTA, 1% BSA, 0.05% CHAPS, pH 7.4, and 0.2% sodium azide) and analyzed by Sandwich ELISAs for A $\beta$ 42 as previously described (Ran *et al*, 2014).

### Biotinylation

Biotinylation experiments were performed to detect cell-surface expression of TREM2 and the AD variants. Briefly, transfected HEK293T cells were incubated with 2 mg/ml sulfo-NHS-biotin (Pierce) in PBS for 30 min on ice. Cells were washed with PBS 100 mM glycine, washed twice with PBS and then lysed in RIPA buffer. Cell lysates were incubated with streptavidin agarose resin (Pierce) overnight at 4°C and washed five times with RIPA buffer and then eluted with protein loading buffer. Eluates were analyzed by Western blot.

### NFAT activation assay

Nuclear factor of activated T-cell (NFAT) activation assay was performed with a GFP reporter as described previously (Wang *et al*, 2015). The 2B4 reporter cell lines transfected with TREM2-IRES-DAP12 or TREM R47H-IRES-DAP12 were incubated with A $\beta$ 42 oligomers for 12 h. NFAT signaling activation was measured by the expression of GFP which was analyzed by flow cytometry. Reporter activity is presented as percentage of cells that express GFP.

### Statistical analysis

Statistics were performed with GraphPad Prims (CA, USA) version 7. Details on specific tests used are providing in the Figure legends.

**Expanded View** for this article is available online.

**The paper explained****Problem**

Triggering receptor expressed on myeloid cells 2 (TREM2) is a member of the immunoglobulin superfamily highly expressed in microglial cells. Rare coding variants of TREM2 (R47H, R62H) are associated with increased risk for Alzheimer's disease (AD), but how they confer this risk remains uncertain.

**Results**

We assessed binding of TREM2, AD-associated TREM2 variants and select TREM family members to various forms of A $\beta$  and APOE in multiple assays. TREM2 interacts directly with various forms of A $\beta$  in multiple assays, with highest affinity interactions observed between TREM2 and soluble A $\beta$ 42 oligomers. AD-associated TREM2 variants bind various forms of A $\beta$  with similar affinity as WT TREM2. High-affinity binding of TREM2 to A $\beta$  oligomers (KD < 1e-12) is characterized by very slow dissociation. Pre-incubation with A $\beta$  oligomers is shown to block the lower affinity interaction of APOE. Our data show that mouse Trem2, Trem1 and Trem1 show the same high-affinity interaction with A $\beta$  oligomers as human TREM2. In cellular assays, AD-associated variants of TREM2 reduced the amount of A $\beta$ 42 internalized, and in NFAT reporter assay, the R47H and R62H variants decreased NFAT signaling activity in response to A $\beta$ 42.

**Impact**

These studies identify a high-affinity interaction between TREM2 and A $\beta$  that can block interaction with another ligand, APOE. These data link TREM2 to physical interactions with two key molecules in Alzheimer's disease, A $\beta$  and APOE, and suggest that partial loss of function of TREM2 mediates increased risk for AD.

**Acknowledgements**

This work was supported by NIH grants RO1AG32991 and NIA grant AG046139-01. We thank Dr. Christian Haass for providing the TREM2 plasmid.

**Author contributions**

CBL, SLM, YZ, TBL, PEC, YR, and TEM performed experiments. CBL, TBL, PC, DMH, JDU, MC, and TEG designed the experiments, reviewed the manuscript, and edited the manuscript drafts. CBL and TEG wrote the manuscript.

**Conflict of interest**

The authors declare that they have no conflict of interest.

**References**

- Atagi Y, Liu CC, Painter MM, Chen XF, Verbeeck C, Zheng H, Li X, Rademakers R, Kang SS, Xu H et al (2015) Apolipoprotein E is a ligand for triggering receptor expressed on myeloid cells 2 (TREM2). *J Biol Chem* 290: 26043–26050
- Bailey CC, DeVaux LB, Farzan M (2015) The triggering receptor expressed on myeloid cells 2 binds apolipoprotein E. *J Biol Chem* 290: 26033–26042
- Bianchin MM, Lima JE, Natel J, Sakamoto AC (2006) The genetic causes of basal ganglia calcification, dementia, and bone cysts: DAP12 and TREM2. *Neurology* 66: 615–616; author reply 615-616
- Carrasquillo MM, Allen M, Burgess JD, Wang X, Strickland SL, Aryal S, Siuda J, Kachadoorian ML, Medway C, Younkin CS et al (2017) A candidate regulatory variant at the TREM gene cluster associates with decreased Alzheimer's disease risk and increased TREM1 and TREM2 brain gene expression. *Alzheimers Dement* 13: 663–673
- Chakrabarty P, Li A, Ceballos-Diaz C, Eddy JA, Funk CC, Moore B, DiNunno N, Rosario AM, Cruz PE, Verbeeck C et al (2015) IL-10 alters immunoproteostasis in APP mice, increasing plaque burden and worsening cognitive behavior. *Neuron* 85: 519–533
- Cheng-Hathaway PJ, Reed-Geaghan EG, Jay TR, Casali BT, Bemiller SM, Puntambekar SS, von Saucken VE, Williams RY, Karlo JC, Moutinho M et al (2018) The Trem2 R47H variant confers loss-of-function-like phenotypes in Alzheimer's disease. *Mol Neurodegener* 13: 29
- Colonna M, Wang Y (2016) TREM2 variants: new keys to decipher Alzheimer disease pathogenesis. *Nat Rev Neurosci* 17: 201–207
- Cruchaga C, Kauwe JS, Harari O, Jin SC, Cai Y, Karch CM, Benitez BA, Jeng AT, Skorupa T, Carrell D et al (2013) GWAS of cerebrospinal fluid tau levels identifies risk variants for Alzheimer's disease. *Neuron* 78: 256–268
- Golde TE, Streit WJ, Chakrabarty P (2013) Alzheimer's disease risk alleles in TREM2 illuminate innate immunity in Alzheimer's disease. *Alzheimers Res Ther* 5: 24
- Hardy J, Selkoe DJ (2002) The amyloid hypothesis of Alzheimer's disease: progress and problems on the road to therapeutics. *Science* 297: 353–356
- Hsieh CL, Koike M, Spusta SC, Niemi EC, Yenari M, Nakamura MC, Seaman WE (2009) A role for TREM2 ligands in the phagocytosis of apoptotic neuronal cells by microglia. *J Neurochem* 109: 1144–1156
- Jay TR, Hirsch AM, Broihier ML, Miller CM, Neilson LE, Ransohoff RM, Lamb BT, Landreth GE (2017) Disease progression-dependent effects of TREM2 deficiency in a mouse model of Alzheimer's disease. *J Neurosci* 37: 637–647
- Jay TR, Miller CM, Cheng PJ, Graham LC, Bemiller S, Broihier ML, Xu G, Margevicius D, Karlo JC, Sousa GL et al (2015) TREM2 deficiency eliminates TREM2+ inflammatory macrophages and ameliorates pathology in Alzheimer's disease mouse models. *J Exp Med* 212: 287–295
- Jiang T, Tan L, Zhu XC, Zhang QQ, Cao L, Tan MS, Gu LZ, Wang HF, Ding ZZ, Zhang YD et al (2014) Upregulation of TREM2 ameliorates neuropathology and rescues spatial cognitive impairment in a transgenic mouse model of Alzheimer's disease. *Neuropsychopharmacology* 39: 2949–2962
- Jiang T, Tan L, Chen Q, Tan MS, Zhou JS, Zhu XC, Lu H, Wang HF, Zhang YD, Yu JT (2016a) A rare coding variant in TREM2 increases risk for Alzheimer's disease in Han Chinese. *Neurobiol Aging* 42: 217. e211–e213
- Jiang T, Zhang YD, Chen Q, Gao Q, Zhu XC, Zhou JS, Shi JQ, Lu H, Tan L, Yu JT (2016b) TREM2 modifies microglial phenotype and provides neuroprotection in P301S tau transgenic mice. *Neuropharmacology* 105: 196–206
- Jin SC, Benitez BA, Karch CM, Cooper B, Skorupa T, Carrell D, Norton JB, Hsu S, Harari O, Cai Y et al (2014) Coding variants in TREM2 increase risk for Alzheimer's disease. *Hum Mol Genet* 23: 5838–5846
- Jin SC, Carrasquillo MM, Benitez BA, Skorupa T, Carrell D, Patel D, Lincoln S, Krishnan S, Kachadoorian M, Reitz C et al (2015) TREM2 is associated with increased risk for Alzheimer's disease in African Americans. *Mol Neurodegener* 10: 19
- Kang SS, Kurti A, Baker KE, Liu CC, Colonna M, Ulrich JD, Holtzman DM, Bu G, Fryer JD (2018) Behavioral and transcriptomic analysis of Trem2-null mice: not all knockout mice are created equal. *Hum Mol Genet* 27: 211–223
- Kleinberger G, Yamanishi Y, Suarez-Calvet M, Czirr E, Lohmann E, Cuyvers E, Struyfs H, Pettkus N, Wenninger-Weinzierl A, Mazaheri F et al (2014) TREM2 mutations implicated in neurodegeneration impair cell surface transport and phagocytosis. *Sci Transl Med* 6: 243ra286
- Kober DL, Alexander-Brett JM, Karch CM, Cruchaga C, Colonna M, Holtzman MJ, Brett TJ (2016) Neurodegenerative disease mutations in TREM2 reveal a functional surface and distinct loss-of-function mechanisms. *Elife* 5: e20391

- Kober DL, Brett TJ (2017) TREM2-Ligand Interactions in Health and Disease. *J Mol Biol* 429: 1607–1629
- Koffie RM, Meyer-Luehmann M, Hashimoto T, Adams KW, Mielke ML, Garcia-Alloza M, Mischeva KD, Smith SJ, Kim ML, Lee VM et al (2009) Oligomeric amyloid beta associates with postsynaptic densities and correlates with excitatory synapse loss near senile plaques. *Proc Natl Acad Sci USA* 106: 4012–4017
- Lee CYD, Daggett A, Gu X, Jiang LL, Langfelder P, Li X, Wang N, Zhao Y, Park CS, Cooper Y et al (2018) Elevated TREM2 gene dosage reprograms microglia responsiveness and ameliorates pathological phenotypes in Alzheimer's disease models. *Neuron* 97: 1032–1048. e1035
- Lill CM, Rengmark A, Pihlstrom L, Fogh I, Shatunov A, Sleiman PM, Wang LS, Liu T, Lassen CF, Meissner E et al (2015) The role of TREM2 R47H as a risk factor for Alzheimer's disease, frontotemporal lobar degeneration, amyotrophic lateral sclerosis, and Parkinson's disease. *Alzheimers Dement* 11: 1407–1416
- Musiek ES, Holtzman DM (2015) Three dimensions of the amyloid hypothesis: time, space and 'wingmen'. *Nat Neurosci* 18: 800–806
- Paloneva J, Autti T, Raininko R, Partanen J, Salonen O, Puranen M, Hakola P, Haltia M (2001) CNS manifestations of Nasu-Hakola disease: a frontal dementia with bone cysts. *Neurology* 56: 1552–1558
- Paloneva J, Manninen T, Christman G, Hovanes K, Mandelin J, Adolfsson R, Bianchin M, Bird T, Miranda R, Salmaggi A et al (2002) Mutations in two genes encoding different subunits of a receptor signaling complex result in an identical disease phenotype. *Am J Hum Genet* 71: 656–662
- Peng Q, Malhotra S, Torchia JA, Kerr WG, Coggeshall KM, Humphrey MB (2010) TREM2- and DAP12-dependent activation of PI3K requires DAP10 and is inhibited by SHIP1. *Sci Signal* 3: ra38
- Pinotsi D, Kaminski Schierle GS, Kaminski CF (2016) Optical super-resolution imaging of beta-amyloid aggregation in vitro and in vivo: method and techniques. *Methods Mol Biol* 1303: 125–141
- Ran Y, Cruz PE, Ladd TB, Fauq AH, Jung JI, Matthews J, Felsenstein KM, Golde TE (2014) gamma-Secretase processing and effects of gamma-secretase inhibitors and modulators on long Abeta peptides in cells. *J Biol Chem* 289: 3276–3287
- Schlepckow K, Kleinberger G, Fukumori A, Feederle R, Lichtenthaler SF, Steiner H, Haass C (2017) An Alzheimer-associated TREM2 variant occurs at the ADAM cleavage site and affects shedding and phagocytic function. *EMBO Mol Med* 9: 1356–1365
- Sims R, van der Lee SJ, Naj AC, Bellenguez C, Badarinarayan N, Jakobsdottir J, Kunkle BW, Boland A, Raybould R, Bis JC et al (2017) Rare coding variants in PLCG2, ABI3, and TREM2 implicate microglial-mediated innate immunity in Alzheimer's disease. *Nat Genet* 49: 1373–1384
- Song W, Hooli B, Mullin K, Jin SC, Cella M, Ulland TK, Wang Y, Tanzi RE, Colonna M (2017) Alzheimer's disease-associated TREM2 variants exhibit either decreased or increased ligand-dependent activation. *Alzheimers Dement* 13: 381–387
- Song WM, Joshita S, Zhou Y, Ulland TK, Gilfillan S, Colonna M (2018) Humanized TREM2 mice reveal microglia-intrinsic and -extrinsic effects of R47H polymorphism. *J Exp Med* 215: 745–760
- Stine WB Jr, Dahlgren KN, Krafft GA, LaDu MJ (2003) In vitro characterization of conditions for amyloid-beta peptide oligomerization and fibrillogenesis. *J Biol Chem* 278: 11612–11622
- Suarez-Calvet M, Araque Caballero MA, Kleinberger G, Bateman RJ, Fagan AM, Morris JC, Levin J, Danek A, Ewers M, Haass C (2016) Early changes in CSF sTREM2 in dominantly inherited Alzheimer's disease occur after amyloid deposition and neuronal injury. *Sci Transl Med* 8: 369ra178
- Tanzi RE (2015) TREM2 and risk of Alzheimer's disease—friend or foe? *N Engl J Med* 372: 2564–2565
- Thornton P, Sevalle J, Deery MJ, Fraser G, Zhou Y, Stahl S, Franssen EH, Dodd RB, Qamar S, Gomez Perez-Nievas B et al (2017) TREM2 shedding by cleavage at the H157-S158 bond is accelerated for the Alzheimer's disease-associated H157Y variant. *EMBO Mol Med* 9: 1366–1378
- Ulrich JD, Finn MB, Wang Y, Shen A, Mahan TE, Jiang H, Stewart FR, Piccio L, Colonna M, Holtzman DM (2014) Altered microglial response to Abeta plaques in APPS1-21 mice heterozygous for TREM2. *Mol Neurodegener* 9: 20
- Ulrich JD, Holtzman DM (2016) TREM2 function in Alzheimer's disease and neurodegeneration. *ACS Chem Neurosci* 7: 420–427
- Wang Y, Cella M, Mallinson K, Ulrich JD, Young KL, Robinette ML, Gilfillan S, Krishnan GM, Sudhakar S, Zinselmeyer BH et al (2015) TREM2 lipid sensing sustains the microglial response in an Alzheimer's disease model. *Cell* 160: 1061–1071
- Wang Y, Ulland TK, Ulrich JD, Song W, Tzaferis JA, Hole JT, Yuan P, Mahan TE, Shi Y, Gilfillan S et al (2016) TREM2-mediated early microglial response limits diffusion and toxicity of amyloid plaques. *J Exp Med* 213: 667–675
- Wunderlich P, Glebov K, Kemmerling N, Tien NT, Neumann H, Walter J (2013) Sequential proteolytic processing of the triggering receptor expressed on myeloid cells-2 (TREM2) protein by ectodomain shedding and gamma-secretase-dependent intramembranous cleavage. *J Biol Chem* 288: 33027–33036
- Yeh FL, Wang Y, Tom I, Gonzalez LC, Sheng M (2016) TREM2 binds to apolipoproteins, including APOE and CLU/APOJ, and thereby facilitates uptake of amyloid-beta by microglia. *Neuron* 91: 328–340
- Yeh FL, Hansen DV, Sheng M (2017) TREM2, microglia, and neurodegenerative diseases. *Trends Mol Med* 23: 512–533
- Yuan P, Condello C, Keene CD, Wang Y, Bird TD, Paul SM, Luo W, Colonna M, Baddeley D, Grutzendler J (2016) TREM2 haploinsufficiency in mice and humans impairs the microglia barrier function leading to decreased amyloid compaction and severe axonal dystrophy. *Neuron* 90: 724–739
- Zhao Y, Wu X, Li X, Jiang LL, Gui X, Liu Y, Sun Y, Zhu B, Pina-Crespo JC, Zhang M et al (2018) TREM2 is a receptor for beta-amyloid that mediates microglial function. *Neuron* 97: 1023–1031. e1027
- Zhong L, Wang Z, Wang D, Martens YA, Wu L, Xu Y, Wang K, Li J, Huang R, Can D et al (2018) Amyloid-beta modulates microglial responses by binding to the triggering receptor expressed on myeloid cells 2 (TREM2). *Mol Neurodegener* 13: 15



**License:** This is an open access article under the terms of the Creative Commons Attribution 4.0 License, which permits use, distribution and reproduction in any medium, provided the original work is properly cited.